Nahrain University, College of Engineering Journal (NUCEJ) Vol.14 No.1, 2011 pp.1-12

Time-Dependent Behavior of Excavation in Cohesive Soils Using the Bounding Surface Model

Dr. Qassun S. Mohammed Shafiqu
Department of Civil Engineering, Nahrain University, Iraq
e-mail: qassun@yahoo.com

Ahmed A. Yassen
Department of Civil Engineering, Nahrain University, Iraq

Abstract

The study was to investigate the behavior of excavation in cohesive soils using the bounding surface model. The model and the finite element formulation are described and verified. Then the ground movements were predicted around an excavation in several types of cohesive soils. The results of the analysis demonstrate the effects of the consolidation process and permeability on the stability of the excavation and that the displacements at excavation boundaries increase with increasing permeability and time but at a lower rate as the permeability value decreased. Also the study shows a significant influence of the critical state parameters on the behavior of excavation in normally consolidated clay comparing with the surface configuration and hardening parameters of the model. Thus the modified Cam-clay model which employs a lower number of parameters can be used for the problems of excavation in normally consolidated clay.

Keywords: consolidation, excavation, finite elements, permeability, plasticity

Introduction

It is generally accepted that the finite element method is the major technique used in numerical analysis of geotechnical problems such as excavation. For example, a coupled finite element analysis with the inclusion of a sequential excavation sequence was developed to predict the displacements around an excavation using the simple elastic soil model [8]. Also the transient stability of excavation in elasto-plastic soils was studied using the Mohr-Coulomb failure criteria [11]. Stability is shown to be a function of the rate of excavation, the soil permeability and the drainage path lengths. Borja [4], presented a numerical model to investigate the influence of fluid flow on the strength and deformation behavior of unsupported and braced excavations using the modified Cam-clay model for representing the soil. Under undrained conditions the sequential excavation and strut installation were simulated in the stratified soil using modified Cam-clay constitutive relationship for modelling Soil nonlinearity [5]. Finite element analyses of unsupported excavations in saturated clay were performed using the elastoplastic bounding surface model [2]. The analyses showed that the model provides a realistic stress distribution within the soil mass around the excavation. A calibrated 2D finite element model using the Lade's double hardening constitutive model for soil was used to form a database of the wall and ground surface movements associated with deep excavation [17]. The results indicated that the cantilever and the lateral bulging excavation stages produce distinctive patterns of ground surface movement profiles.

In the following sections, the proposed model and the finite element formulation are described and examples of model prediction and accuracy of the finite element formulation are given. The behavior of a vertical cut in different cohesive soils is then studied.

Bounding Surface Model

Details of the elastoplastic formulation, the numerical implementation of the model and the parameters associated with the model are available in Dafalias and Herrmann [6]. Therefore, only the elastoplastic rate relations are given here.
The total strain rate is consisting of two parts: elastic strain and plastic strain:

$$\dot{\varepsilon}_{ij} = \dot{\varepsilon}^{e}_{ij} + \dot{\varepsilon}^{p}_{ij} \qquad (1)$$

The inverse form of the constitutive relations is obtained as [6]:

$$\dot{\sigma}_{ij} = D_{ijkl}\,\dot{\varepsilon}_{kl} \qquad (2)$$

$$D_{ijkl} = G\left(\delta_{ki}\delta_{ij} + \delta_{kj}\delta_{ii}\right) + \left(K - (2/3)G\right)\delta_{ij}\delta_{kl} \left[3KF_{,\bar{I}}\delta_{ij} + \frac{G}{J}F_{,\bar{J}}\delta_{ij} + \frac{\sqrt{3}G}{\cos 3\alpha}\frac{F_{,\alpha}}{bJ}\left(\frac{s_{in}s_{nj}}{J^2} - \frac{3S^3 s_{ij}}{2J^4} - \frac{2\delta_{ij}}{3}\right)\right] - \frac{\bar{h}\langle L\rangle}{B}\left[3KF_{,\bar{I}}\delta_{ij} + \frac{G}{J}F_{,\bar{J}}\delta_{ij} + \frac{\sqrt{3}G}{\cos 3\alpha}\frac{F_{,\alpha}}{bJ}\left(\frac{s_{in}s_{nj}}{J^2} - \frac{3S^3 s_{ij}}{2J^4} - \frac{2\delta_{ij}}{3}\right)\right] \quad (3)$$

$$L = \frac{1}{B}\left\{ 3KF_{,\bar{I}}\dot{\varepsilon}_{kk} + \frac{G}{J}F_{,\bar{J}}s_{ij}\dot{\varepsilon}_{ij} + \frac{\sqrt{3}G}{\cos 3\alpha}\frac{F_{,\alpha}}{bJ}\left[\left(\frac{s_{ik}s_{kj}}{J^2} - \frac{3S^3 s_{ij}}{2J^4}\right)\dot{\varepsilon}_{ij} - \frac{2\dot{\varepsilon}_{kk}}{3}\right]\right\} \quad (4a)$$

$$B = K_p + 9K\left(F_{,\bar{I}}\right)^2 + G\left(F_{,\bar{J}}\right)^2 + G\left(F_{,\alpha}/bJ\right)^2 \quad (4b)$$

and where K and G represent the elastic bulk and shear moduli, respectively, δ_{ij} is the Kronecker delta, K_p the plastic modulus, I and J are the stress invariants, $1 \le b \le \infty$ and F represents the analytical expression of the bounding surface.

The material parameters used to operate the bounding surface plasticity model are [12]: $\lambda =$ slope of consolidation line, $\kappa =$ slope of swelling line, $N(\alpha) =$ slope of critical state line, $N_c = N$ in compression, $N_e = N$ in extension, $R(\alpha) = R > 1$ defines the point $I_1 = I_o / R$ (Figure, 1), which together with point J_1 define the coordinates of point H which is the intersection of $F = 0$ and CSL, $R_c = R$ in compression, $R_e = R$ in extension, $A(\alpha) =$ parameter defines the distance $D = AI_o$ of apex H of the hyperbola from its center G intersection of the two asymptotes, $A_c = A$ in compression, $A_e = A$ in extension, $T = I_t / I_o$ parameter which determines the purely tensile strength of the material, $C = 0 \le C < 1$ parameter which determines the center of the bounding surface $I_c = CI_o$. $s =$ parameter which determines indirectly "elastic nucleus". For $s = 1$ the elastic nucleus degenerates to point I_c center of bounding surface and as $s \to \infty$ the elastic nucleus expand towards the bounding surface. $h =$ slope-hardening factor, which is a function of lode angle (α),

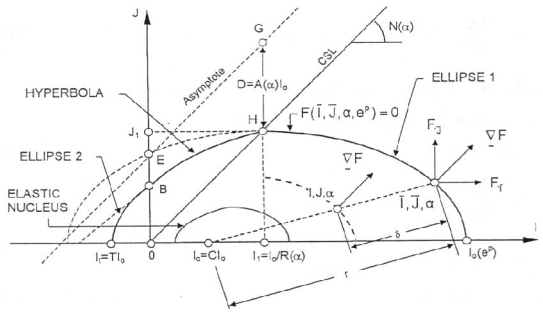

Fig. 1: Bounding surface in stress invariants space [6].

Finite Element Formulation

The elastoplastic bounding surface model described above is incorporated in a finite element program **EXCBS**, which has the feature of modeling two-dimensional geotechnical problems such as consolidation, multistage excavation, written by FORTRAN90 language. This program is primarily based on the programs presented for the analysis of one and a two-dimensional solid by finite element method utilizing elastic constitutive relationship [13] which is modified for the purpose of this study. The flow chart of the computer program is shown in Figure (2). And the typical input and output for the program are given in Appendix (I).

Extensive modifications and newly added subroutines were found necessary to develop a program **EXCBS** incorporating or carrying out the following:

1. Elastoplastic bounding surface model which has the features that plastic deformation may occur for stress state within the surface.
2. Biot consolidation (or the ability of taking the effects of dissipation of pore water pressure with time).
3. Excavation technique, by applying the excavation load to the boundary of excavation to get stress free boundaries.
4. Initial stress algorithm instead of initial strain one.
5. General program permitting any shape of initial mesh.
6. General program with multiple property groups if required.

7. Subroutines of mesh-exc.f90, dis-exc.f90, vec-exc.f90 have been developed to generate postscript output files of the deformed, the undeformed mesh, and the nodal displacement vectors, respectively.

Description of all of the program features is beyond the scope of this paper, and a brief summary of the features relevant to this study is given here.

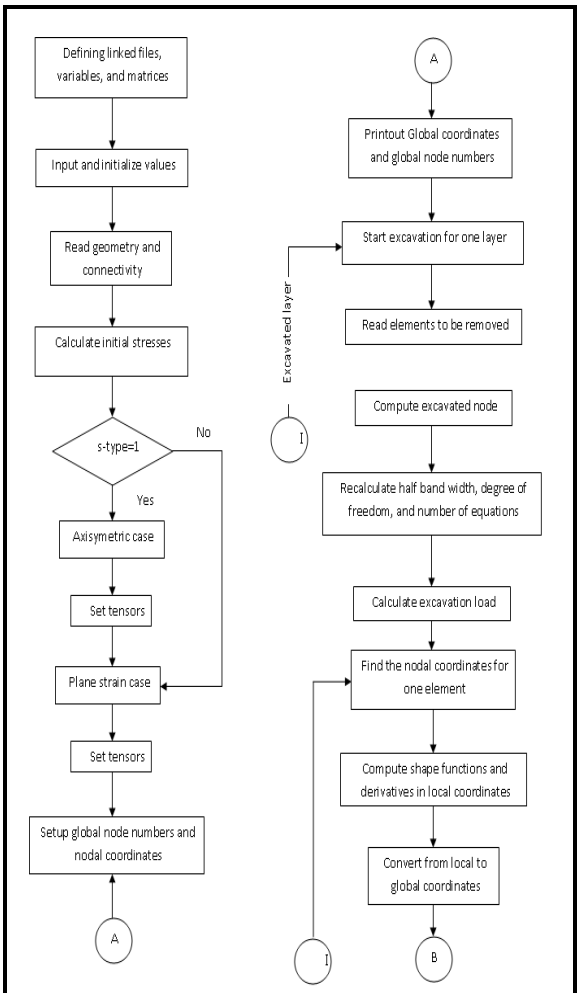

Fig. 2: Flow chart for the program **EXCBS.**

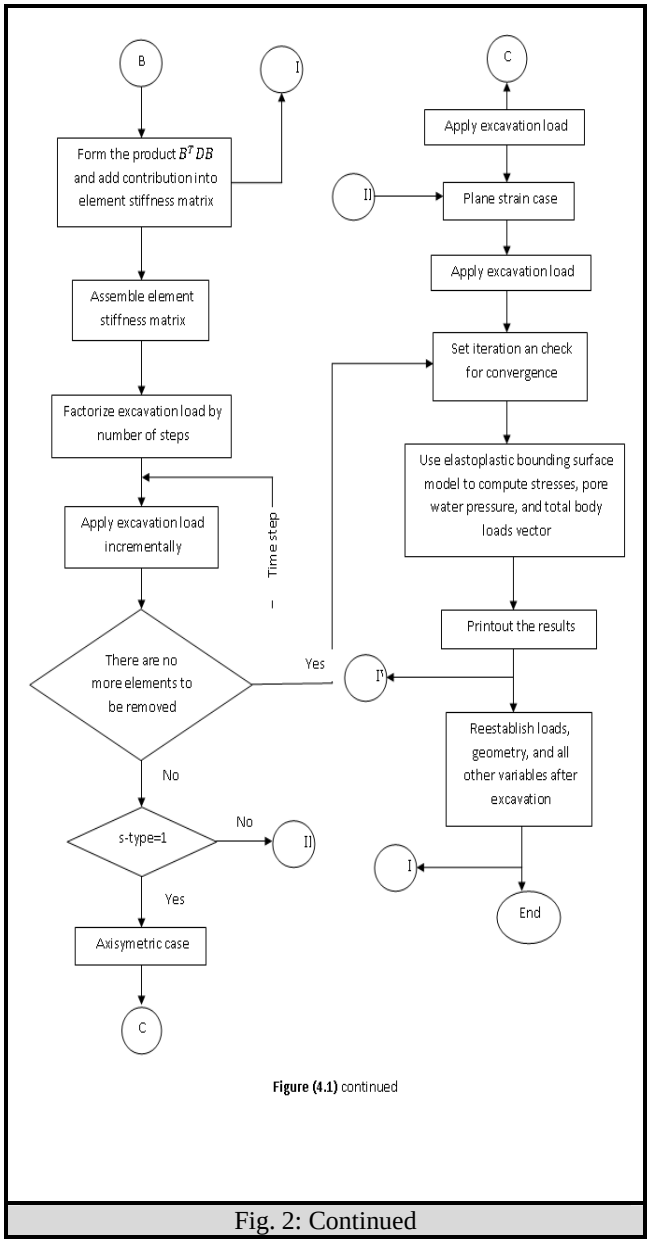

Fig. 2: Continued

Excavation Algorithm

When a portion of material is excavated, either in open excavations or an enclosed tunnel, forces must be applied along the excavated surface such that: (1) The new "free surface" is stress free, and (2) The bounding forces at the i^{th} stage of an excavation are given as [14]:

$$F_i = \int_{Vi} B^T \sigma_{i-1} dV - \int_{Vi} N^T \gamma \, dV \qquad (5)$$

where B is the strain-displacement matrix, N the element shape functions. The first term is the nodal internal resisting force vector due to the stresses in the removed elements, and the second term the reversal of the nodal body-load forces (of the removed elements) assuming that γ (the body-load due to gravity) is acting downwards. Also the total stress in eq.(5) was obtained by adding the effective stress computed at the Gauss points from the solid phase of the analysis (8-node), to the pore pressures interpolated from their nodal values of the fluid phase (4-node).

Transient Formulation

In the case of an excavation, the loading is time-dependent, so an incremental formulation was used in the following work producing the matrix version of the Biot equation at the element level presented below [11].

$$\begin{bmatrix} K & L \\ L^T & S+\overline{\alpha}H\Delta t_k \end{bmatrix}\begin{Bmatrix}\overline{u}\\ \overline{p}\end{Bmatrix}=\begin{bmatrix} K & L \\ L^T & S-(1-\overline{\alpha})H\Delta t_k \end{bmatrix}\begin{Bmatrix}\overline{u}\\ \overline{p}\end{Bmatrix} + \begin{Bmatrix} dF/dt+C \\ \overline{F}\end{Bmatrix} \quad (6)$$

where: K = element solid stiffness matrix, L = element coupling matrix, H = element fluid stiffness matrix, $\overline{u}$ = change in nodal displacements, $\overline{p}$ = change in nodal excess pore-pressures, S = the compressibility matrix, $\overline{F}$ = load vector, Δt = calculation time step, $\overline{\alpha}$ = time stepping parameter (=1 in this work), dF/dt = change in nodal forces.

Verification Problems

Transient Analysis of Excavation in Elastic soils

The analysis was performed on the single column of elements in Fig. 3. The soil was assumed to be elastic and initially stress free and have the drained properties shown in Fig. 3.

Removing the top element and allowing the column to drain show, the distribution of non-dimensional excess pore pressures throughout the column, Fig.4. The obtained results are for different values of the time factor T_v, where H is the drainage path (after excavation),which is equal to 15m in this case. The results are well compared with those from the analytical and numerical solutions [15,8].

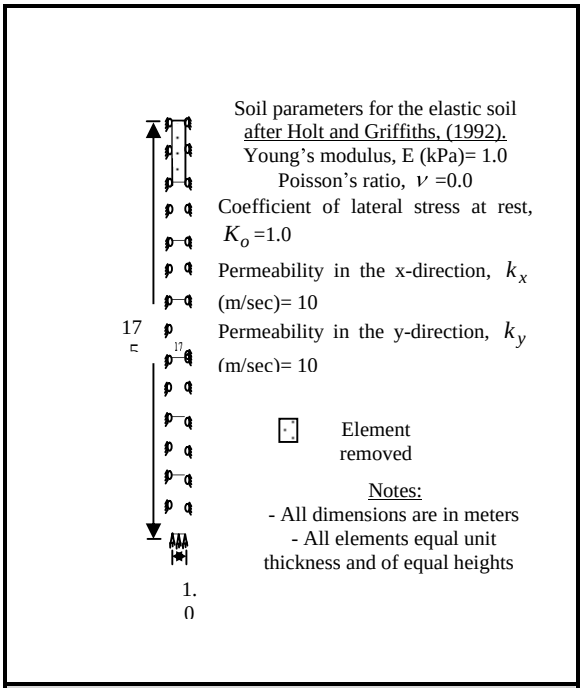

Fig. 3: Finite element mesh for the one-dimensional excavation problem.

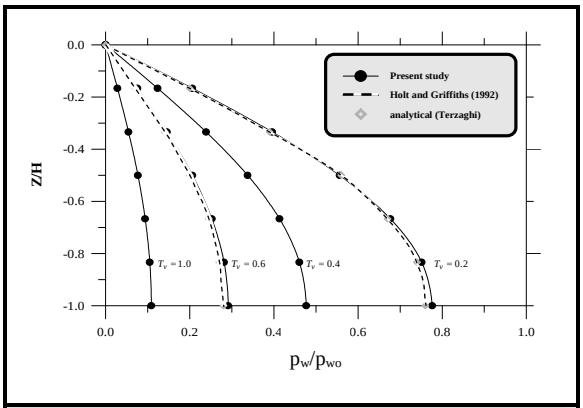

Fig. 4: Excess pore pressure

Elastoplastic Analysis of Two-Dimensional Consolidation Problem

Fig. 5 shows the finite element mesh used; the width of the loaded area, b, is assumed equal to (3.05m). The problem is solved using the input material parameters shown in Table 2. Fig.6 shows time wise variation of surface settlements, using the modified Cam-clay and bounding surface models. It can

be seen that the settlement values obtained by the two models do not differ significantly at the early stage of time levels. However, at later times the

bounding surface plasticity results show higher settlements but a smaller final settlement. Also the figure shows that the results of bounding surface model from the present study are compared well with those of Al-Ebady [1].

Table 2: Bounding surface parameters (after Siriwardane and Desai, 1981;Al-Ebady, 2001).

parameters	Value	parameters	Value
λ	0.14	A_e	0.08
κ	0.05	C	0.4
υ	0.4	s_p	1.0
M_c	1.05	h_c	4.0
M_e	0.89	h_e	4.0
R_c	2.72	h_o	4.0
R_e	2.18	m	0.02
A_c	0.1	k (m/day)	1.22×10^{-5}

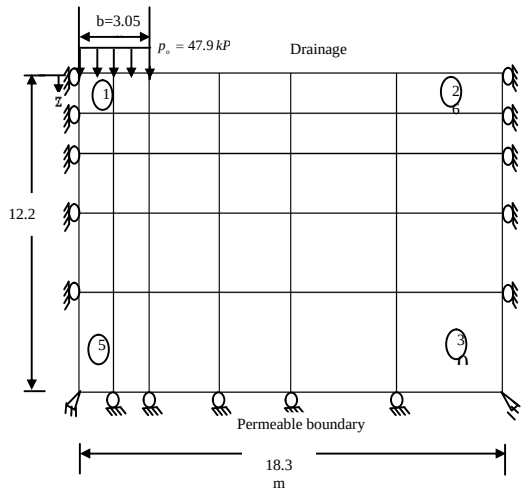

Fig. 5: Finite element mesh for the two-dimensional consolidation problem.

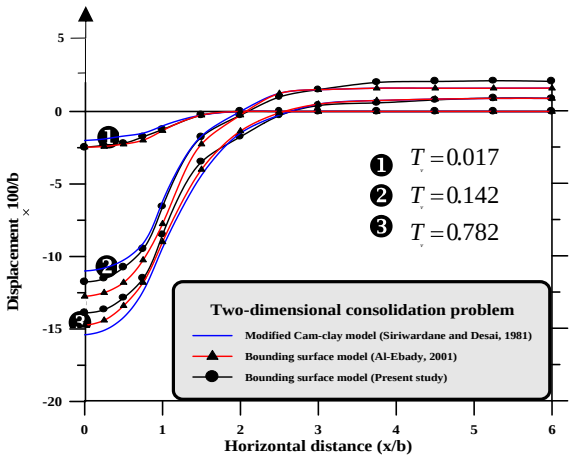

Fig. 6: Surface settlements versus horizontal distance at three different time values.

Finite Element Analysis of Excavations in Several Types of Cohesive Soil

The finite element mesh representing the problem is illustrated in Fig. 7. This is the same problem previously considered to show the ability of the bounding surface model to solve the consolidation problems but with different parameters of the model according to the type of cohesive soil [10]. The parameters are tabulated in Table 3, where the parameters S_p, a *and* w are fixed for all the types of soils as 1, 1.2 and 5 respectively. Here a 6.1m side by 5.34m deep excavation is made in order to remove the 9 elements on top left side of the mesh (Fig. 7) where the dotted elements represent the elements removed during excavation. In the analysis, three values of permeability k were considered which are 1.22×10^{-4} m/day, 1.22×10^{-6} m/day and 1.22×10^{-8} m/day typically for normally to overconsolidated clays [3]. The excavation rate will be taken equal to 0.25m/day, thus the excavation will be completed in 25days or time factor of $T_v = 0.07$. The top element was removed and the column was allowed to drain for different values of the non-dimensional time factor T_v given by:

$$T_v = c_v t / H^2 \qquad (7)$$

where t is the time, H is the drainage path in the vertical direction (at the end of excavation) and c_v the coefficients of consolidation in the vertical direction as defined by:

$$c_v = \frac{k(1-\nu)E}{(1-2\nu)(1+\nu)\gamma_w} \quad (8)$$

values of the Poisson's ratio ν for the five types of cohesive soils are given in Table 3, knowing that for the undrained case the value of ν is 0.5 which gives an infinite values for c_v and T_v. Thus a value of ν equal to 0.49 will be numerically acceptable for the undrained case.

The results were obtained at the end of excavation when the time factor $T_v = 0.07$ and after 100 days or time factor $T_v = 0.278$. In the following sections, analysis of the unsupported excavation is carried out in order to study the effects of the consolidation process, permeability and the bounding surface model parameters on the excavation stability.

Table 3: Bounding surface parameters for the five cohesive soils [10]

Parameters / Soil type	λ	κ	υ	M_c	M_e	R_c	R_e	A_c	A_e	C	h_c	h_e
Kaolin mix	0.075	0.011	0.22	1.35	0.9	3.05	1.71	0.18	0.15	0.49	11	9.6
Kaolin	0.14	0.05	0.2	1.05	0.85	2.65	2.25	0.02	___[a]	0.7	4	5.6
Marine silty clay	0.178	0.052	0.2	1.07	0.79	2.2	___[a]	0.1	___[a]	0.4	10	10
Grenoble clay	0.2	0.1	0.15	0.78	0.8	2.5	2	0.02	0.02	0.5	4.3	4.3
Umeda clay	0.343	0.105	0.15	0.77	0.61	2.39		0.01	___[a]	0.2	2	___[a]

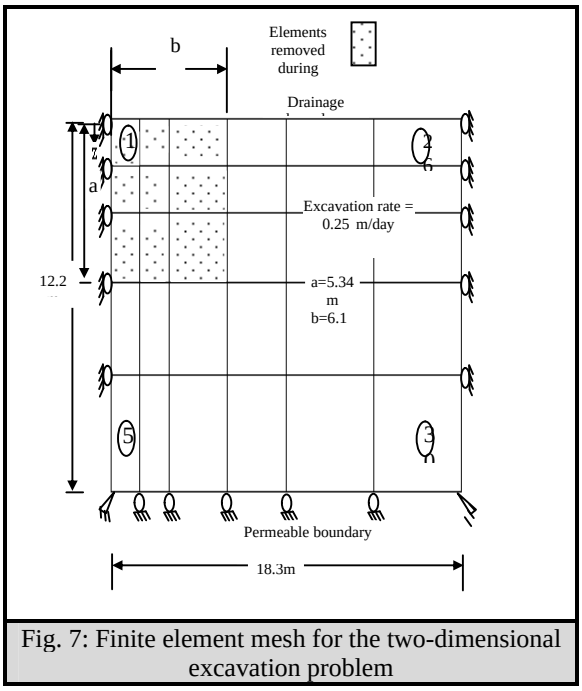

Fig. 7: Finite element mesh for the two-dimensional excavation problem

Effect of the permeability and consolidation process

Figs. 8 and 9 show the normalized displacements for the five different soil types for the three different permeability values at the end of excavation and at the time factor $T_v = 0.278$. The normalization will give an indication for the behavior of excavation in different depth and width. As it can be noticed that the lateral movement of the vertical wall and the dredge line heave increased with increasing the permeability and time but at a lower rate as the permeability value decreased. This may be attributed to the fact that For higher permeability clay (i.e., $k = 1.22 \times 10^{-4}\ m/day$), little excess pore pressures contours exist at the end of excavation since the excavation rate is slow enough to allow dissipation to occur. While for the lower permeability clay (i.e., $k = 1.22 \times 10^{-8}\ m/day$), large negative excess pore water pressures were developed after excavation. The excess pore pressures dissipated with time, due to the water flow towards the opening thus causing increase in the lateral displacement and heave of the vertical and horizontal boundaries of the excavation region, respectively. Significant movements with time occur in higher permeability clay with time as the dissipation of excess pore pressures is at high rate in

these soils comparing with that in lower permeability clay.

Also, when excavation carried out in higher permeability clay the displacements at the crest of cut which can be taken as an indication of the failure of excavation is increased by about 15% to 20% than that in lower permeability clay at the end of excavation. These percentages increased with time and reach approximately 25% to 30% when the time is increased by a factor of four. Finally, there are insignificant differences between the displacements for the clays of low and very low permeability values (i.e, $k = 1.22 \times 10^{-6}$ and $k = 1.22 \times 10^{-8}\ m/day$, respectively) at the end of excavation. On the other hand, the difference will appear clearly with time reaching the increase in crest displacement in lower permeability clay after increasing time by a factor of four to about 5% to 15% than that in very low permeability clay which remains almost constant.

Influence of the bounding surface parameters

Fig. 10 shows the lateral displacement and heave of the vertical and horizontal boundaries of excavation region, and for the five soil types. The results were taken for the case when the time factor is $T_v = 0.278$ and for a higher value of permeability (i.e., $k = 1.22 \times 10^{-4}\ m/day$) in order to recognize the effects of the parameters clearly.

In general, it was observed that for cohesive soils that have higher values of the model parameters λ and κ and lower values of $M, \nu, R, h, A \text{ and } C$, higher lateral displacement of the vertical boundary and basal heave were noticed for the excavation region. Also, lower displacements around the cut after excavation were predicted for Kaolin Mix that has the lowest values of λ and κ, and the highest values of $M, \nu, R, h \text{ and } A$ with a larger amount of the projection center *C*.

In order to recognize the most effective parameters that influence the behavior of the excavation, a parametric study is carried out by, first, changing the values of each of the parameters $M, \nu, R, h, A \text{ and } C$ for the Umeda clay and keeping λ and κ constant, then, keeping the origin values of $M, \nu, R, h, A \text{ and } C$ for the Umeda clay constant, and decreasing the values of λ and κ. It was indicated that the critical state parameters λ and κ are the most effective parameters compared with others as shown in Figs 11 and 12. The displacements will be reduced with a higher percent by decreasing the values of λ and κ, while increasing the values of the parameters $M, \nu, R, h, A \text{ and } C$ will show little increase in the results of displacements comparing with those using the original parameters.

The reason for the insignificant influence of the parameters $M, \nu, R, h, A \text{ and } C$ on the displacements may be due to the fact that, the excavation is carried out in normally consolidated clay (i.e., OCR=1) where the values of these parameters are not operational since the point lies on (F=0) and thus they are related to the response for overconsolidated states [6].

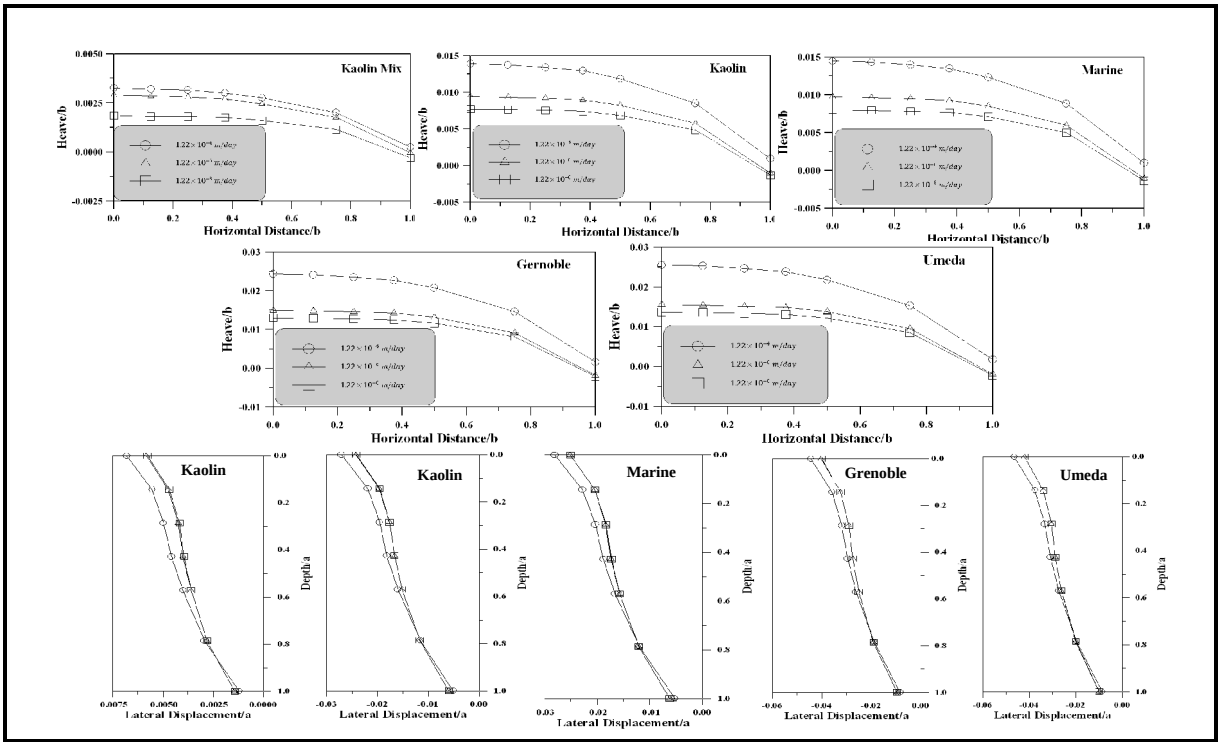

Fig. 8: Dredge line heave and lateral movement of vertical wall of the excavation in several cohesive soils for different permeability values at the end of excavation

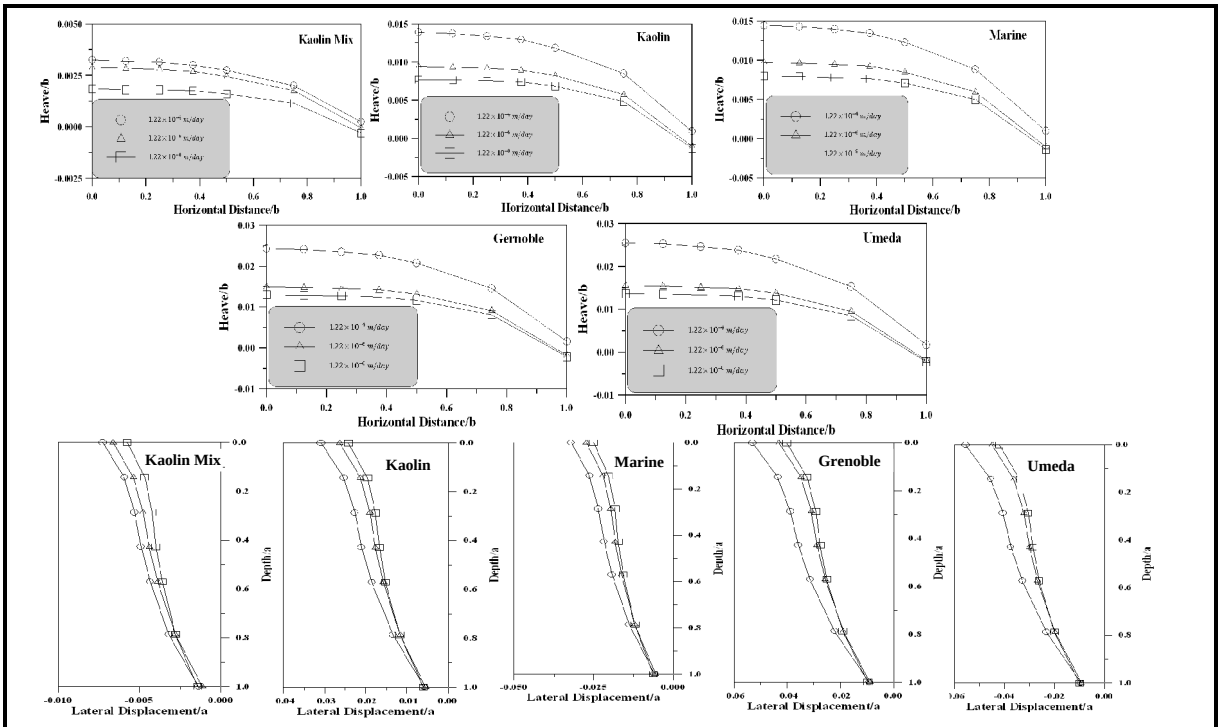

Fig. 9: Dredge line heave and lateral movement of vertical wall of the excavation in several cohesive soils for different permeability values at the time factor ($T_v = 0.278$)

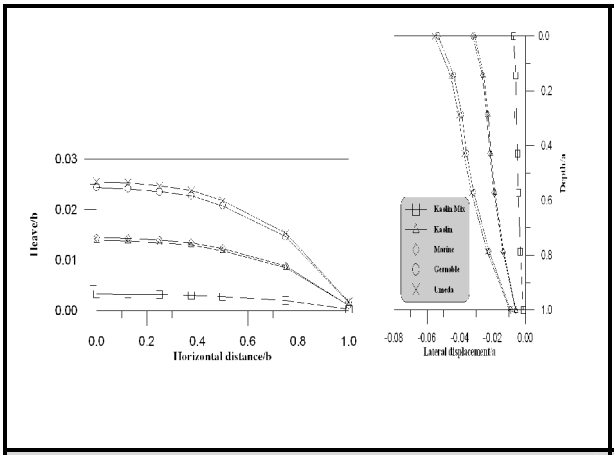

Fig. 10: Lateral displacement and heave of the excavation boundaries in the cohesive soils

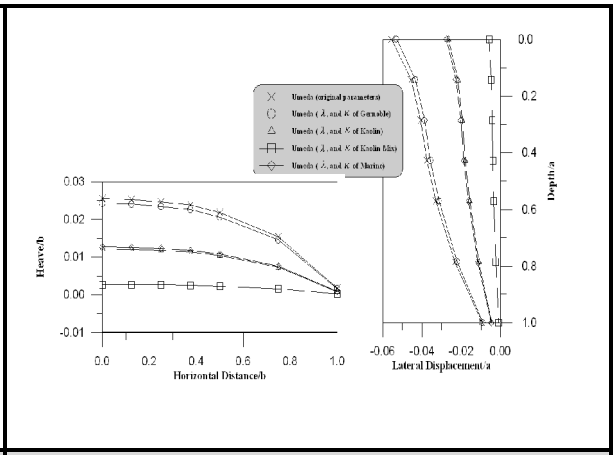

Fig. 11: Lateral displacement and heave of the excavation boundaries in Umeda clay with variable values of M, ν, R, h, A *and* C

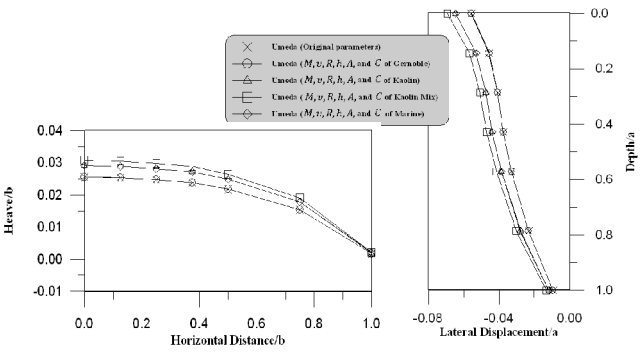

Fig. 12: Lateral displacement and heave of the excavation boundaries in Umeda clay with variable values of λ and κ.

Conclusions

The following conclusions are drawn from the present study:

1. For higher permeability clays, little excess pore pressures contours exist at the end of excavation as the excavation rate is slow enough to allow dissipation to occur.
2. The lateral movement of the vertical wall and the dredge line heave increased with increasing the permeability and time but at a lower rate as the permeability value decreased. It was observed that the displacement at the crest of the cut in higher permeability clay is greater by approximately 15% t0 20% than that in lower permeability clay at the end of excavation, and this percent is increased with time to reach about 25% to 30%, when the time is increased by a factor of four.
3. There were insignificant differences between the displacements for clays of low and very low permeability values at the end of excavation. The differences appear clearly with time reaching the increase of crest displacement in lower permeability clay after increasing time by a factor of four to about 5% to 15% than that in very low permeability clay which remains almost constant.
4. In cohesive soils that have higher values of the model λ and κ and lower values of M, ν, R, h, A *and* C higher lateral displacement of the vertical boundary of the excavation region and basal heave were predicted. Also, increasing the values of

the parameters M, ν, R, h *and* A and lowering λ and κ will cause lower displacements around the cut after excavation.

5. The study shows significant influence of the critical state parameters λ and κ on the behavior of excavation in normally consolidated clay compared with the parameters M, ν, R, h, A *and* C. Thus the modified Cam clay model which employs a lower number of parameters can be used for the problems of excavation in normally consolidated clay instead of bounding surface model.

References

[1] A. S. Al-Ebady, "Consolidation using bounding surface plasticity model," M.Sc. Thesis, University of Baghdad,2001.

[2] F. A. Al-Jumaily, and Q. S. Mohammed Shafiqu, "Finite element analysis of the unsupported excavation using the elastoplastic bounding surface model," Proceedings of the International Conference on Geotechnical Engineering, Beirut,pp. 192-198, 2004.

[3] J. P. Bardet, "Experimental soil mechanics," Prentice Hall , New Jersey , 1997.

[4] R. I. Borja, "Free boundary, fluid flow, and seepage forces in excavations," Journal of Geotechnical Engineering, Vol. 118, No. 1, pp. 125-146, 1992.

[5] S. K. Bose, and N. N. Som, "Parametric study of a braced cut by finite element method," Computers and Geotechnics, Vol. 22, Issue 2, pp. 91-107, 1998.

[6] Y. F. Dafalias, and L. R. Herrmann, "Bounding surface plasticity II:Application to isotropic cohesive soils," Journal of Engineering Mechanics, ASCE, Vol. 112, No. 12, pp.1263-1291, 1986.

[7] M. Dysli, and A. Fontana, "Deformations around the excavations in clay soil," In Proceedings of International Symposium on Numerical Models in Geomechanics, Zurich.Edited by R.Durger and J.A. Studer, pp. 634-642, 1982.

[8] D. A. Holt, and D. V. Griffiths, "Transient analysis of excavations in soil," Computers and Geotechnic, Vol. 13, pp. 159-174, 1992.

[9] V. N. Kaliakin, "Parameter estimation for time-dependent bounding surface models. Geo-Frontiers conference (2005); Soil constitutive models: evaluation, selection, and calibration," Geotechnical special publication No.128, pp. 237-256, 2005.

[10] V. N. Kaliakin, and Y. F. Dafalias, "Details regarding the elastoplastic-viscoplastic bounding surface model for isotropic cohesive soils," Civil Engineering Report No.91-1, University of Delaware, Newark, 1991.

[11] R. W. Lewis, and B. A. Schrefler, "The finite element method in the deformation and consolidation of porous media," John Wiley and Sons Ltd., London, 1987.

[12] H. J. Siriwadane, and C. S. Desai, "Two numerical schemes for nonlinear consolidation," International Journal for Numerical Methods in Engineering, Vol. 17, pp. 405-426, 1981.

[13] I. M. Smith, and D. V. Griffiths, "Programming Finite Element Method," 3rd Ed., John Wiley and Sons, 1998.

[14] I. M. Smith, and D. V. Griffiths, "Programming Finite Element Method," 4th Ed., John Wiley and Sons, 2004.

[15] K. Terzaghi, "Theoretical soil mechanics," John Wiley and Sons Ltd.,1943.

[16] A. E. Osaimi, and G. W. Clough, "Pore-pressure dissipation during excavation," ASCE Journal of the Geotechnical Engineering Division, Vol. 105(GT4), pp. 481-498, 1979.

[17] C. Yoo, and D. Lee, "Deep excavation-induced ground surface movement characteristics – A numerical investigation," Computers and Geotechnic, article in press, 2007. doi:10.1016/j.compgeo.2007.05.002.

Appendix I

Typical input and output of the program **EXCBS** for the excavation problem in Grenoble clay and for the permeability value of 1.22×10^{-4} m/day, after 100 days or time factor $T_v = 0.278$:

Input:

30,113,4,1.,1.,.75,.001,250,1.
2
2
1

1
1
1.22.e-4,1.22.e-4,-----,1.22.e-4,
.0000E+00 .0000E+00
-
-
.183E+02 -.122E+02
21 14 1 2 3 15 23 22
23 15 3 4 5 16 25 24
25 16 5 6 7 17 27 26
-
-
109 98 89 90 91 99 111 110
111 99 91 92 93 100 113 112
93
1,0,1,0,
2,1,1,0
-
-,
112,0,0,0,
113,0,0,0
1
100
9
1 2 3 7 8 9 13 14 15

Output:

The total number of elements is 30
The total possible number of equations is: 208
Global coordinates
Node 1 .0000E+00 .0000E+00
-
-
Node 113 .183E+02 -.122E+02
Global node numbers
Element 1 21 14 1 2 3 15 23 22
Element 2 23 15 3 4 5 16 25 24
-
-
Element 29 109 98 89 90 91 99 111 110
Element 30 111 99 91 92 93 100 113 112

Time step 100

no. of Excavated elements= 9

Their numbers 1 2 3 7 8 9 13 14 15
Steering vector
element 1 0 0 146 147 130 131 133 134 0 135 0 148 0 0 0 0 0 132 136 0
element 2 0 0 146 147 130 131 133 134 0 135 0 148 0 0 0 0 0 132 136 0
-
-
There are 148 freedoms and nband is 50 in step 100
The excavation load in lift 1 is .4751E+03

The time is .1000E02
Lift number 1 gravity load increment 100
It took 3 iterations to converge

Displacements (m) and epwp (kPa):
Node No. displ(x) displ(y) epwp
Node 7 .92962E+00 .46889E+00 .10000E+03
Node 8 .73128E+00 .10950E+00 .10000E+03
node 9 .54482E+00 .50406E-01 .10000E+03
-
-
Stresses (kPa):
SX SY SZ SXY pw
========== element
10 .2439E+03 .4706E+03 .4469E+03 -.1495E+02 -.1232E+00
-
-
Element 30 .5379E+03 .4537E+03 .5479E+03 .6121E+01 -.4742E+00

التصرف الزمني للحفريات في الترب الطينية باستخدام نموذج السطح المحيط

د. قاسيون سعدالدين محمد شفيق **احمد اكرم ياسين**

قسم الهندسة المدنية، جامعة النهرين، العراق

الخلاصة

الدراسه الحاليه هي لبحث تصرف الحفرة في الترب الطينيه باستخدام نموذج السطح المحيط. النموذج وقوانين طريقة العناصر المحدده تم شرحها وتدقيقها. ثم تم ايجاد الازاحات حول الحفرة في عده انواع من الترب الطينيه. نتائج التحليل اظهرت تاثيرات عملية الانضمام والنفاذية على استقراريه الحفرة وان الازاحات عند حدود الحفرة تزداد بزيادة النفاذية والزمن ولكن بنسب تقل مع نقصان قيم النفاذية. ايضا الدراسة اظهرت التاثير الواضح لمعاملات الحاله الحرجة على تصرف الحفر في الترب الطينية طبيعيه الانضمام مقارنة مع تاثير معاملات ترتيب السطح ومعاملات التصلب للنموذج. لهذا فان نموذج (Cam-Clay) المعدل والذي يستخدم معاملات اقل يمكن استخدامها في مسائل الحفر في الترب الطينيه طبيعيه الانضمام.